Appl. Phys. A 74, 19–25 (2002) / Digital Object Identifier (DOI) 10.1007/s003390100893

**Applied Physics A**
Materials
Science & Processing

# Femtosecond laser ablation of silicon–modification thresholds and morphology

**J. Bonse***, **S. Baudach**, **J. Krüger**, **W. Kautek**, **M. Lenzner**

Laboratory for Thin Film Technology, Federal Institute for Materials Research and Testing (BAM), Unter den Eichen 87, 12205 Berlin, Germany

Received: 4 December 2000/Revised version: 29 March 2001/Published online: 20 June 2001 – © Springer-Verlag 2001

**Abstract.** We investigated the initial modification and ablation of crystalline silicon with single and multiple Ti:sapphire laser pulses of 5 to 400 fs duration. In accordance with earlier established models, we found the phenomena amorphization, melting, re-crystallization, nucleated vaporization, and ablation to occur with increasing laser fluence down to the shortest pulse durations. We noticed new morphological features (bubbles) as well as familiar ones (ripples, columns). A nearly constant ablation threshold fluence on the order of 0.2 J/cm$^2$ for all pulse durations and multiple-pulse irradiation was observed. For a duration of $\approx 100$ fs, significant incubation can be observed, whereas for 5 fs pulses, the ablation threshold does not depend on the pulse number within the experimental error. For micromachining of silicon, a pulse duration of less than 500 fs is not advantageous.

**PACS:** 79.20D; 42.70.Q

Micromachining with ultrashort laser pulses has attracted growing interest even in industry and medicine since the appropriate lasers were made readily available for a wide set of parameters [1, 2]. It has been demonstrated that ultrashort pulses bear the potential for precise micromachining (laterally and vertically) in transparent dielectrics [3]. In the course of investigations with femtosecond pulses, it became obvious that the detailed mechanisms of damage to solids caused by laser light are far from fully understood.

A number of phenomena concerning photo-induced modification of silicon surfaces have been explored in different ranges of wavelength, intensity and duration of the applied laser pulses. In this paper, we want to extend the existing investigations on laser-induced surface damage in silicon to pulse durations as short as 5 fs. We also observed several different phenomena; we try to methodically "file" these observations into a physical overview.

We will demonstrate that the so-far-assumed sequence of physical processes, namely amorphization [4], melting [5, 6], re-crystallization [4, 7], nucleated vaporization [8], and finally ablation [9], can also account for these experimental results. Various well-known features, for example, ripples [10] and columns [11], could be realized and appropriately explained as well. In Sect. 1, the current knowledge about the interaction between laser pulses and silicon is reviewed. Our experimental results are shown and compared to this in Sect. 2.

## 1 Physical considerations

The deposition of the laser energy into a solid is usually viewed in the quantum-mechanical formalism of particle interaction. The incident pulse energy is absorbed by the electrons, dependent on the peak intensity, by one-, two- or more-photon absorption. Absorption by free carriers (sometimes called inverse bremsstrahlung) depends on the number of already existing carriers and is therefore a subsequent process. The same applies to collisional ionization, which utilizes part of the energy of highly excited carriers to generate new free electrons. These carriers then thermalize to a Fermi–Dirac distribution while transferring their excess energy to phonons, typically on a time scale of 100 fs. These phonons afterwards recombine to a Bose–Einstein distribution in a few picoseconds [12]. During the detailed exploitation of pulsed-laser annealing (PLA, typically done with nanosecond pulses), a "plasma-annealing" model was established, which stated that a non-thermal "bond softening" was responsible for the loss of the crystal structure [13, 14]. Recently, this non-thermal model was shown to be applicable for several semiconductors irradiated with femtosecond pulses [15–18].

So far, no spatial transport of energy out of the excitation region has been considered. In order to treat the subsequent processes, including melting, boiling, and ablation of material, one usually uses either a two-temperature model [19, 20], which distinguishes between electron and lattice (ion) temperatures, or a completely classical model of thermal transport in a continuum [8, 21]. The latter one describes phase changes from the molten phase to a gas, considering the existence of transient thermodynamical states (such as superheated liquids) due to the rapid action of the ultrashort laser pulses.

The physical mechanisms that are involved in photo-excitation of the solid are manifested also in irreversible

*Corresponding author.
(Fax: +49-30/8104-1827, E-mail: joern.bonse@bam.de)

changes of the irradiated surface. These changes can be used for identification of some of the processes and also for determination of their threshold fluences.

After irradiation with short laser pulses, re-solidification of molten material was observed to happen in two stages: amorphization and re-crystallization [4]. The difference was simply attributed to the amount of energy deposited in the material (the temperature) and the consequent cooling velocity. At lower temperatures, the material has not enough time to re-crystallize from the melt, thus leaving the semiconductor in an amorphous state. In regions with higher temperatures, cooling is sufficiently slow to allow re-crystallization.

Already in previous experiments, a rather mysterious phenomenon has been discovered after the solids have been irradiated with multiple subsequent pulses [22]. Finally termed "ripples", these periodic surface structures appear as lines orthogonal to the direction of the electric field vector of the incident light and show a period on the order of the wavelength of the generating light [10, 23]. The generally accepted explanation of these ripples is an interference between the incident light and a surface wave (generated by scattering). This interference leads to periodic modulation of the absorbed intensity and consequently to modulated ablation.

Column formation in crystalline silicon as a result of multi-pulse laser irradiation has been observed in the past at different laser wavelengths (UV–NIR), for different pulse durations (fs–ns), and in different environments (vacuum, air, different gases). A certain number of laser pulses is required to initiate the self-organized growth process of Si microcolumns in the irradiated region. This phenomenon is of major importance because it can limit the precision of laser ablation. For the treatment with ultrashort (fs) laser pulses, the Si-column formation was observed by several groups under different experimental conditions ($\lambda = 248$ nm, $\tau = 105$ fs, vacuum [24]; $\lambda = 390$ nm, $\tau = 250$ fs, vacuum [9]; $\lambda = 620$ nm, $\tau = 300$ fs, air [25]; $\lambda = 780$ nm, $\tau = 100$ fs, $SF_6$, $Cl_2$, $N_2$, He, vacuum [11]). The phenomenon was also found for short-pulse (ns) excimer-laser irradiation ($\lambda = 193$ nm, $\tau = 23$ ns, air [26]; $\lambda = 248$ nm, $\tau = 25$ ns, $SF_6$, $N_2$, $O_2$, Ar [27]; $\lambda = 248$ nm, $\tau = 12$ ns, vacuum [28]; $\lambda = 308$ nm, $\tau = 28$ ns, vacuum [29]).

The process strongly depends on the number of pulses applied to the same spot and the laser fluence. A further key parameter for the formation process and the shape of the microstructures seems to be the ambient environment. Oxidizing or halogen-containing atmospheres such as air, $O_2$ or $SF_6$ support the generation of high-aspect-ratio pillars, whereas the formation of sharp spikes can be reduced in vacuum, $N_2$ or He [11]. On the other hand, column formation is rather insensitive to the laser wavelength [9, 11, 24, 25] and the pulse duration [30, 31]. Influences of the doping concentration have not been observed [11, 27]. For these reasons, a chemical control of the dimensions of microcolumns seems to be possible [31].

## 2 Experimental results and analysis

Experiments were carried out with two different Ti:sapphire laser systems, a commercial CPA system (SPECTRA PHYSICS, Spitfire) at the BAM Berlin and the Vienna system, comprised of an amplifier and hollow fiber compressor, which is capable of producing 5-fs pulses with a maximum energy of 500 μJ [32]. The pulse duration of the latter one was changed between 5 fs and 400 fs by inserting dispersive material (glass blocks) in the beam path. The experimental conditions were kept similar. The center wavelengths of the linearly polarized laser pulses differed by only 20 nm (BAM: 800 nm, Vienna: 780 nm). The different repetition rates (BAM: 10 Hz, Vienna: 1 kHz) should have no influence on the experimental results because every physical process known to be important here is terminated after 1 ms. An important measurement – actually the one that dominates the overall error – is the energy detection. Here we used a pyroelectric detector BESTEC PM200 (BAM) and the OPHIR pulse energy detector NOVA (Vienna), respectively.

Different pulse numbers with varying energy were focused to a diameter on the order of several 10 μm (BAM: $f = 60$ mm plano-convex lens, Vienna: $R = 100$ mm spherical silver mirror) onto the polished (111) surface of $n$-doped silicon samples. On these samples, a native oxide layer of about 2.7 nm thickness has been found from ellipsometric measurements. For higher applied fluences (in the single-pulse case for 5-fs pulses), the sample was placed in a slightly evacuated chamber ($p \approx 10^{-4}$ mbar) in order to prevent ionization or non-linear effects in air and resulting pulse distortions.

Inspection of the irradiated surface regions was performed using an optical microscope (Reichert–Jung, Polyvar) in Nomarski mode. A more detailed characterization of morphological changes of the laser-modified areas was done by means of a scanning electron microscope (SEM) equipped with a cold-field electron emission cathode (Hitachi, S-4100, accelerating voltage 10 kV) and an atomic force microscope (AFM, Digital Instruments, Dimension 3000 SPM) operated in tapping mode.

Anticipating the results of our investigations, we outline the principal physical processes occurring on the Si surface after a Gaussian laser pulse was incident in Fig. 1. For comparison, a damage spot on the silicon surface generated by a single laser pulse is shown in Fig. 2 exhibiting different circular regions of modification, annealing, and ablation. The formation of ripples cannot be seen in this picture because it only occurs after irradiation with multiple pulses onto the same sample spot. In the following section, these thresholds will be further investigated and classified quantitatively.

### *2.1 Modification thresholds*

Some of the early experiments on laser-induced modification of silicon surfaces distinguish regions of amorphization and crystallization [4]. We observed the same phenomena in our experiments, but the zone of amorphization showed a further substructure which we believe is related to oxidation of the surface layers of silicon. The thresholds of oxidation and amorphization are so close together that unambiguous identification is hardly possible. However, in order to take this fact into account, we call the physical process in this region modification rather than amorphization.

The threshold fluences for these phenomena can be determined similar to the ablation threshold fluence, namely measuring the diameter of the modified areas versus the pulse fluence and extrapolating to zero [33]. In Fig. 3, the square of

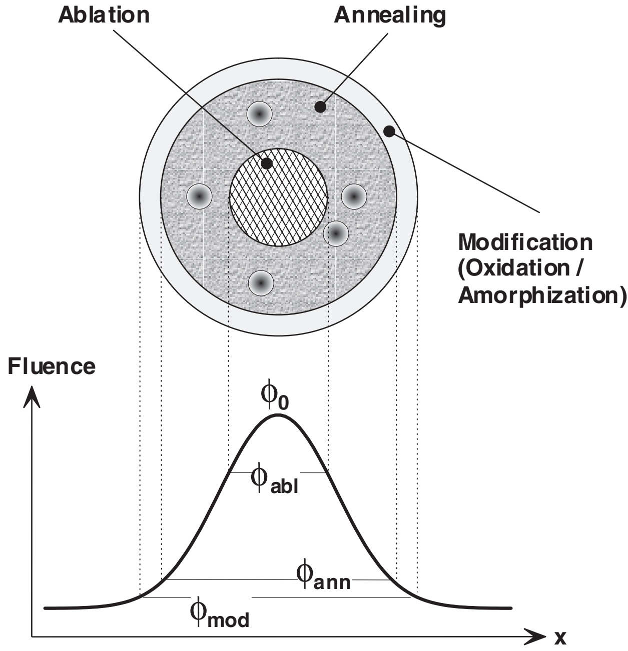


**Fig. 1.** Physical processes during the modification of silicon with femtosecond laser pulses and their threshold fluences

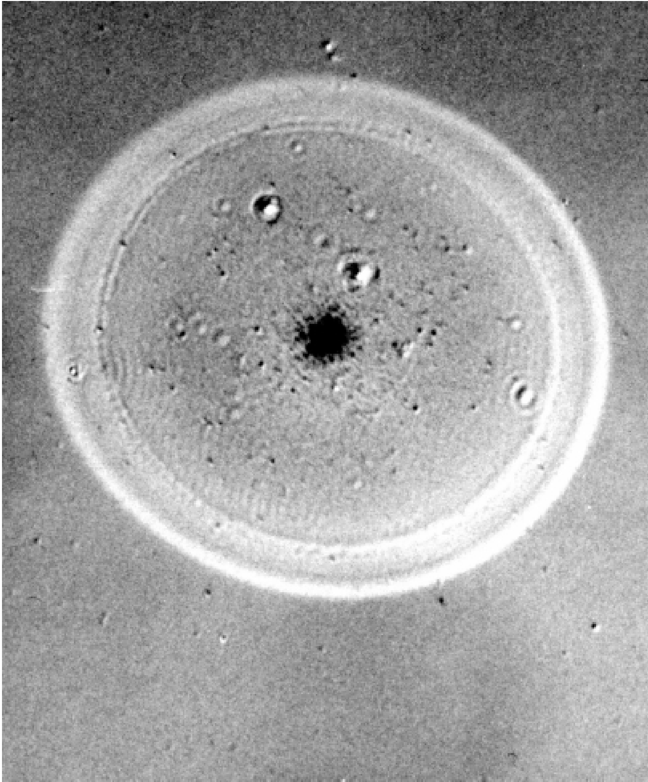

**Fig. 2.** Nomarski optical micrograph of the silicon sample surface treated with a single laser pulse in air ($\lambda = 800$ nm, $\tau = 130$ fs, $\Phi_0 = 1.5$ J/cm$^2$). The outermost ring has a diameter of 45 μm

the diameter (corresponding to a modified area) is depicted versus increasing peak fluence of the laser pulses. Extending the regression of this line to zero yields the threshold values to $\Phi_{\text{mod}} = 0.26\,\text{J/cm}^2$ and $\Phi_{\text{ann}} = 0.55\,\text{J/cm}^2$, respectively. For the applied pulse duration, this is identical to the single-pulse threshold measured by Pronko et al. [20].

The ablation thresholds of multi-shot experiments in air for different pulse durations are shown in Fig. 4. For pulse durations below 100 fs, the threshold becomes constant, a behavior that is well known for metals [34].

For higher pulse numbers, one can find no more evidence for crystallization or oxidation/amorphization. A clean edge of ablation as in Fig. 9a can be recognized. From the dimensions of these craters, an ablation threshold is determined which cannot be distinguished from other thresholds due to morphological changes in the irradiated surface region.

The values in Fig. 4 are significantly lower than the single-pulse thresholds evaluated from Fig. 3, because the thresholds of modification and ablation depend on the number of applied laser pulses. This incubation effect rests on a non-ablating modification of the sample material by the laser pulses in such a manner that the threshold for damage decreases. This effect has been extensively studied at the surface of single-crystal metals [35]. A dependence in the form of a power law was found:

$$\Phi_{\text{mod}}(N) = \Phi_{\text{mod}}(1) \cdot N^{\xi-1}. \tag{1}$$

$\Phi_{\text{mod}}(N)$ denotes the modification threshold fluence for $N$ laser pulses, and $\xi$ is a material-dependent coefficient. Incubation is related to an accumulation of energy (i.e. non-complete dissipation of the deposited energy) into plastic stress–strain of the metal. However, this formula has also successfully been employed in the case of indium phosphide (InP) [36], where it is unclear whether intermediate storage of laser energy is mechanical or, for example, chemical (as in several glasses by F-center formation [37]). In Fig. 5, the dependence of $N \cdot \Phi_{\text{mod}}(N)$ on the number of pulses is plotted for our data. The fit according to (1) (solid line) yields a coefficient $\xi$ of 0.84.

From Fig. 5, one can conclude that there is significant incubation in silicon for pulses with a duration of $\approx 100$ fs.

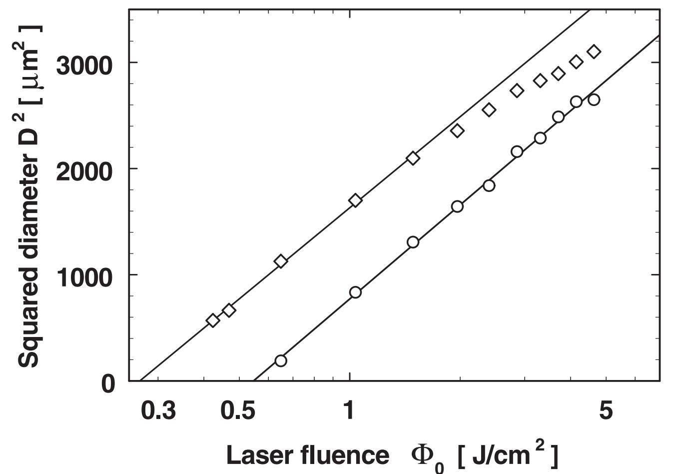


**Fig. 3.** Diameter (squared) of modification and re-crystallization of the silicon surface versus the incident peak fluence of the laser pulse ($\lambda = 800$ nm, $\tau = 130$ fs, $N = 1$, in air). *Squares* belong to the areas of modification, whereas *circles* belong to the re-crystallization regions. *Solid lines* are linear regressions within the semi-logarithmic plot. The deviation of the data from the regression for high fluences is attributed to a slightly non-Gaussian beam profile (caused by apertures)

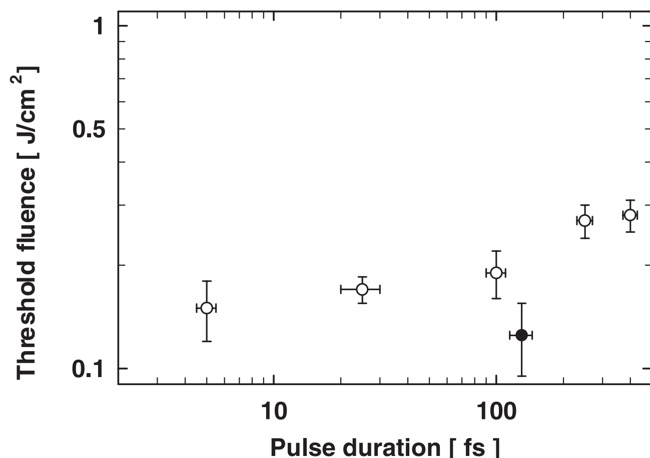


**Fig. 4.** Ablation threshold fluence of n-Si(111) for several pulse durations, 100 pulses per spot, in air. Values measured at $\lambda = 780$ nm, except the *solid circle* ($\lambda = 800$ nm)

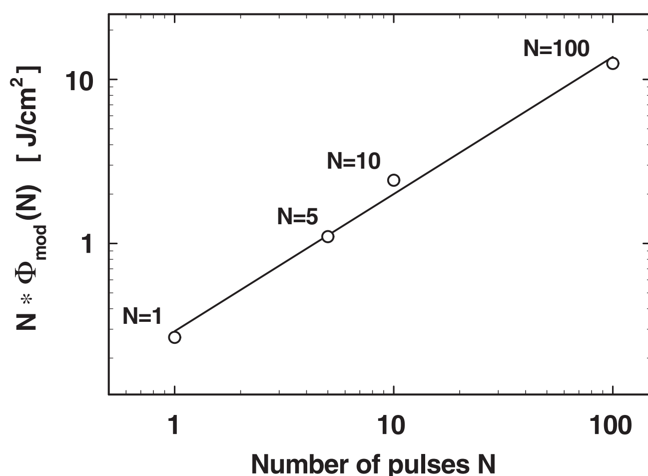


**Fig. 5.** Threshold fluence of laser-induced damage of silicon versus number of laser pulses with a duration of $\tau = 130$ fs and $\lambda = 800$ nm in an air environment. The *solid line* represents a least-squares-fit with (1), where $\xi = 0.84$

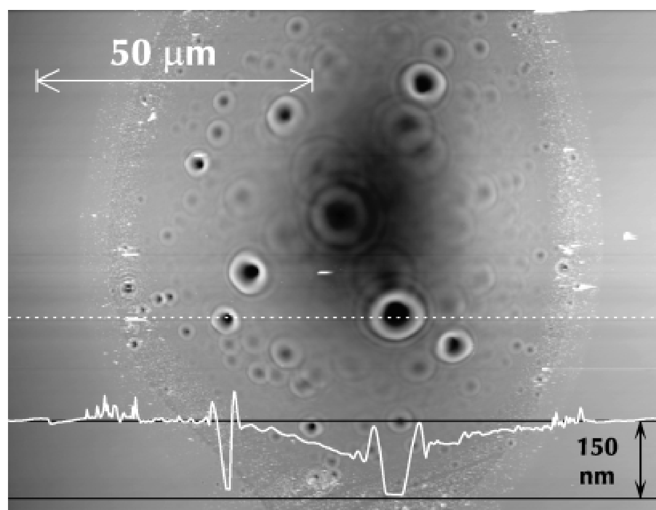


**Fig. 6.** AFM picture of damage in silicon generated with a single Ti:sapphire laser pulse ($\lambda = 780$ nm, $\tau = 5$ fs, $\Phi_0 = 7.7$ J/cm$^2$). *Dark areas* indicate more ablated material. The *inset* at the bottom of the picture is a line-scan along the *dotted white line*, the depth scale is indicated in *black*

The precise nature of this effect, whether energy is stored in the form of chemical modification or by mechanical stress (as in the case of metals), cannot be deduced from these results.

Interestingly, single-shot measurements with 5-fs pulses yield a damage threshold of $0.20 \pm 0.05$ J/cm$^2$, which agrees with the threshold achieved with multiple pulses within the experimental error (compare Fig. 4). Obviously – for these short pulses – there is no such intermediate storage of energy below the damage threshold as it was found, for example, in fused silica [38].

### *2.2 Single-pulse experiments*

Surface images taken with an atomic force microscope (AFM) and a scanning electron microscope (SEM) reveal interesting morphological features of the damaged areas. The

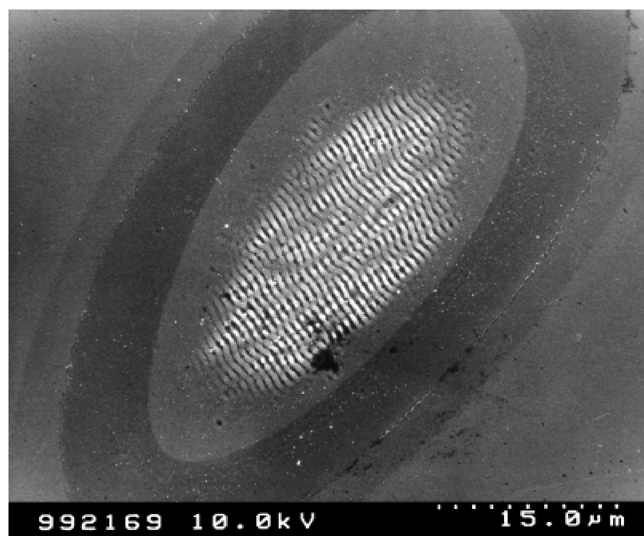


**a**

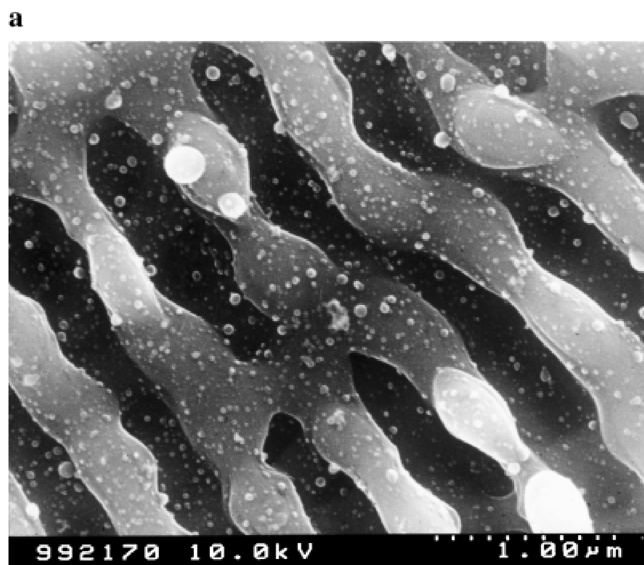


**b**

**Fig. 7a,b.** SEM picture (0°) of damage in silicon generated with Ti: sapphire laser pulses in air ($\lambda = 780$ nm, $\tau = 5$ fs, $\Phi_0 = 2.5$ J/cm$^2$, $N = 5$). Three different regions of modification (ablation including ripples, recrystallization, and amorphization) can be recognized. **a** Full view, **b** detail

formation of circular substructures (holes) within the cavities can be observed (see Fig. 6). These holes vanish or are obscured by other morphological features when the same spot is illuminated with subsequent pulses. With increasing laser fluence, the size of these holes increases. Phenomena such as these are frequently attributed to a locally enhanced carrier density generated either by an inhomogeneous laser beam profile or by locally enhanced absorption (scratches, crystal defects, dust).

An initialization of inhomogeneous surface structures due to "hot spots" in the beam profile can be ruled out because – due to the efficient spatial filtering by guiding in a hollow fiber – the Vienna system exhibits an extremely smooth beam profile [32].

External surface impurities (dust, scratches due to polishing) cannot be significant, as we will see in the following argument. We consider indirect two-photon absorption with a coefficient of only 1 cm/GW [39] as the dominant carrier-generating mechanism. Calculating the penetration depth induced by this mechanism, one finds that the number of absorbing atoms in the excited volume is far smaller than the number of photons supposedly absorbed in this volume. Thus, even the indirect two-photon absorption is already strongly saturated. Virtually all available electrons are excited and it is hardly conceivable that the carrier density exhibits local spikes (e.g. by absorption of defects) so distinct that locally enhanced ablation could occur.

Although an enhancement of surface absorption is no appropriate explanation for the observed substructures, enhancement of absorption at depth in the semiconductor (where the light intensity already dropped one or more orders of magnitude) could account for an evolving inhomogeneous energy deposition.

Consequently, after the strongly saturated and overheated surface layer was removed by phase explosion, normal boiling including inhomogeneous nucleation of bubbles occurs in the remaining liquid layer [21]. This scenario is supported by the fact that larger bubbles are formed in regions of higher fluences, i.e. regions of higher temperature (and therefore slower cooling) where bubbles have more time to grow.

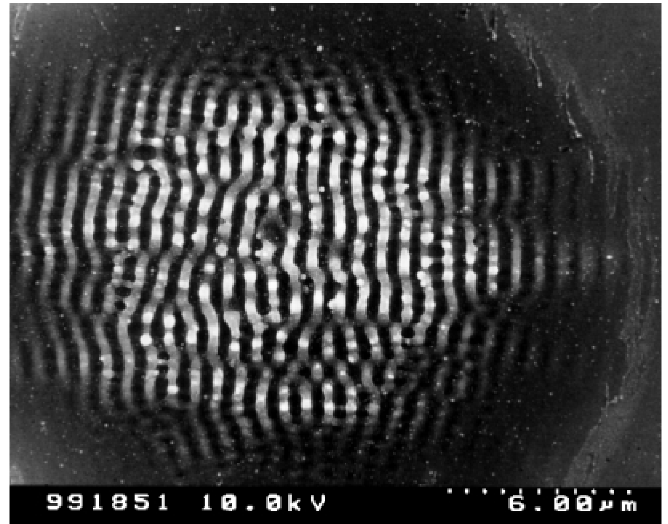


**Fig. 8.** SEM picture (0°) of damage in silicon generated with Ti:sapphire laser pulses in air ($\lambda = 800$ nm, $\tau = 130$ fs, $\Phi_0 = 0.42$ J/cm$^2$, $N = 5$)

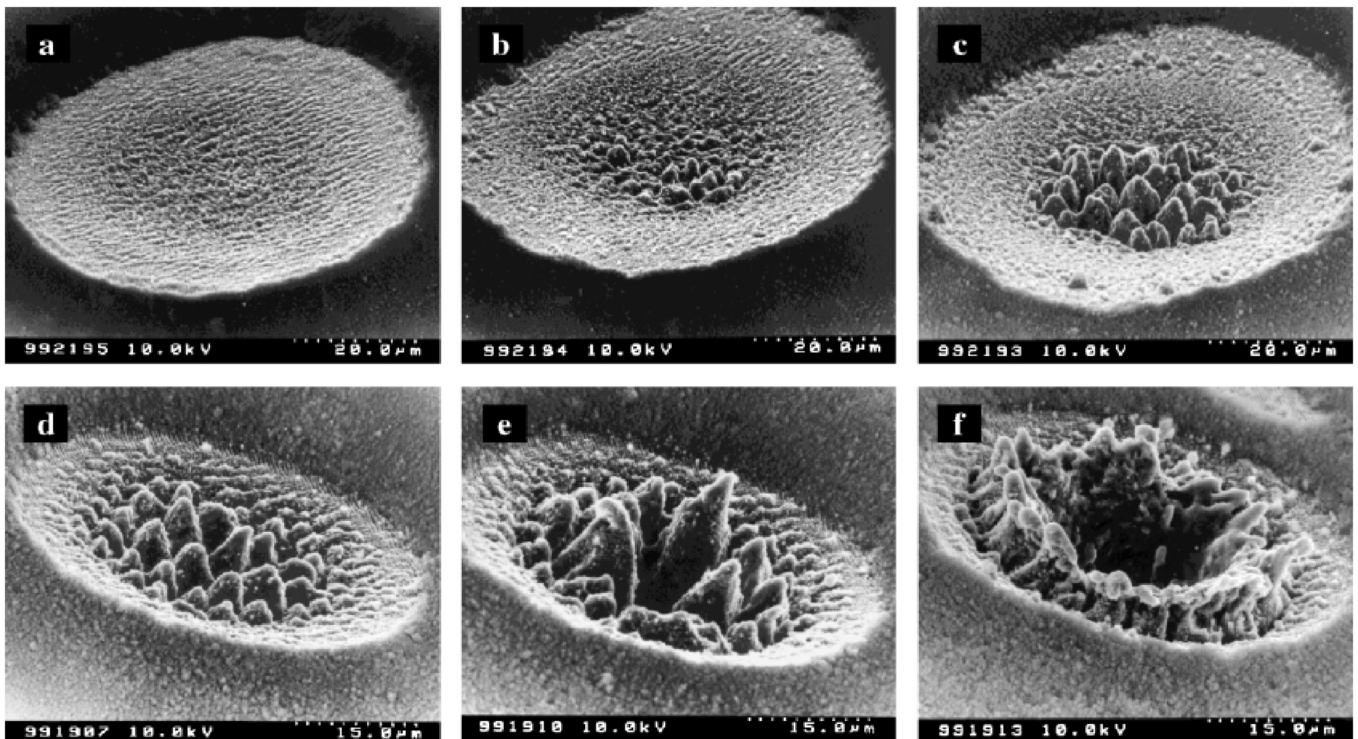


**Fig. 9a–f.** SEM pictures (60°) of damage in silicon generated with Ti:sapphire laser pulses in air. **a** $\Phi_0 = 1.0$ J/cm$^2$, **b** 1.3 J/cm$^2$, **c** 1.8 J/cm$^2$ ($\lambda = 780$ nm, $\tau = 100$ fs, $N = 100$). **d** $\Phi_0 = 2.0$ J/cm$^2$, **e** 2.8 J/cm$^2$, **f** 4.1 J/cm$^2$ ($\lambda = 800$ nm, $\tau = 130$ fs, $N = 100$)

*2.3 Ablation with multiple pulses*

The application of a moderate number ($N \approx 5$) of laser pulses leads to characteristic laser-induced periodic surface structures (ripples). In single-pulse experiments, these highly oriented structures were not observed, indicating that a feedback mechanism is involved during the formation of the surface patterns. Fig. 7 shows typical surface damage in silicon ($\lambda = 800$ nm, $\tau = 5$ fs) at a fluence of 2.5 J/cm$^2$. Three different modified zones are clearly visible (compare Fig. 1): ablation and ripple-formation in the central region, annealing in the first annular structure, and modification in the outer annular border. It is interesting to note, that all these surface modifications known from longer pulses also occur at this ultrashort pulse duration of 5 fs. A magnified view (Fig. 7b) reveals average lateral ripple periods between 650 nm and 750 nm which is comparable to the laser wavelength. The ripples were always oriented perpendicular to the electric-field vector of the incident radiation. Thus, we attribute this phenomenon to the well-known mechanism of interference and subsequent local field enhancement [10]. Small globules of re-deposited material were observed on the top of the surface corrugations.

The same characteristic ripple morphology was detected in the central crater region at an $\approx 25$ times longer pulse duration ($\lambda = 800$ nm, $\tau = 130$ fs, $\Phi_0 = 0.42$ J/cm$^2$, $N = 5$, see Fig. 8). Additionally, some outspread periodic patterned (triangular) regions are seen in the direction of the electric field.

A further increased number of laser pulses ($N \approx 100$) leads to another characteristic surface morphology: the columns or pillars, already introduced in Sect. 1. A certain pulse number is required to nucleate the column growth process. The evolution of silicon microcones and mirocolumns in a series of laser-generated craters, obtained with a constant number of 100 Ti:sapphire laser pulses ($\tau = 100$ fs at $\lambda = 780$ nm, and $\tau = 130$ fs at $\lambda = 800$ nm) at varying peak fluences in air is shown in Fig. 9.

At a comparatively low fluence of 1.0 J/cm$^2$ (which is $\approx 5-6$ times above the ablation threshold), a uniformly ablated crater with a rough, but featureless bottom can be seen as well as highly directed nearly wavelength-sized ripple structures in the border region (Fig. 9a). With increasing laser fluence, small conical structures arise from the bottom of the craters to form the initial stages of microcolumns (Fig. 9b,c). The lateral and vertical extent of the columns and the spacing between them strongly depends on the local fluence. In the center of the irradiated area, the columns are wider, taller and more sparse. In the border region they are packed closer together. Up to a fluence of $\approx 2$ J/cm$^2$, the columns are formed in the middle of the crater (Fig. 9d), while at higher fluences ($\Phi_0 = 2.8$ J/cm$^2$) the morphology appears crown-like. At this stage of development, the columns can protrude above the original surface plane (Fig. 9e), which provides conclusive evidence for the redeposition/re-crystallization origin of these columns. At further increased laser fluences of $\Phi_0 \approx 4.1$ J/cm$^2$, a volcano-like structure is observed within the ablated region (Fig. 9f). It is probably formed by not completely ejected material, which is redeposited at the crater walls when the crater depth exceeds a certain value. The height of the columns grows with an increasing number of laser pulses. If a critical size is reached, a destruction of the Si pillars occurs [24].

Concerning the formation mechanism of the silicon columns, we suggest a similar explanation as Lowndes et al. [31]. Initial surface corrugation inhomogeneously nucleates from local vaporization (bubble ejection from the melt layer) and/or ripple formation and subsequently re-deposited material. On the edges of these corrugations, the absorbed local laser fluence is reduced due to an altered angle of incidence of the laser radiation. Therefore, ablation takes place preferably at the minima and maxima of the surface topography. The silicon-rich vapor which is formed at the grooves cools during the material transport (expansion of the vapor plume) and can be re-deposited at the protruding features of the surface. During a large number of these transport cycles, a highly protruding column can be formed. Additionally, the effect can be enhanced by multiple reflections of the incident laser radiation on the bodies of the columns,

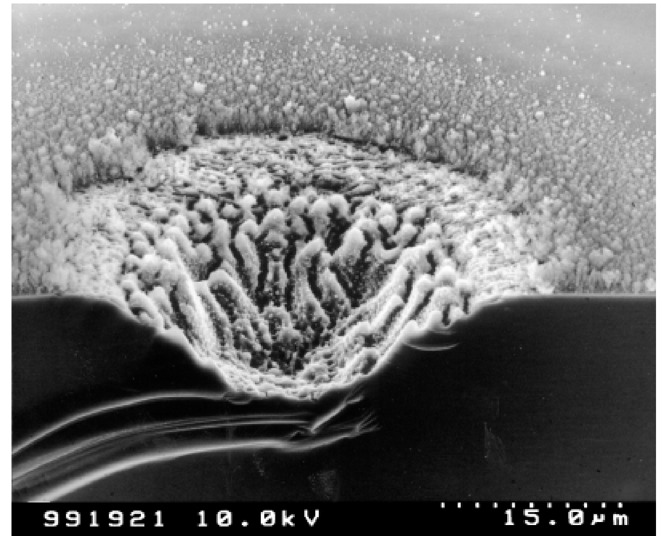


**a**

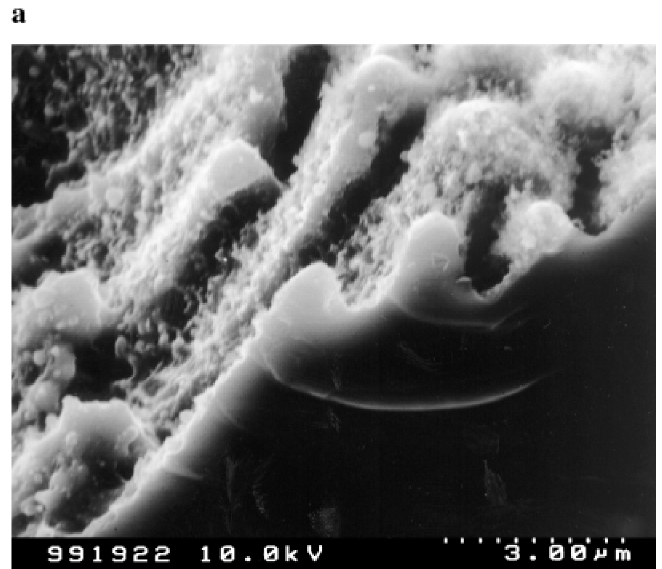


**b**

**Fig. 10a,b.** Cross-sectional SEM picture of damage in silicon generated with Ti:sapphire laser pulses in air ($\lambda = 800$ nm, $\tau = 130$ fs, $\Phi_0 = 0.65$ J/cm$^2$, $N = 500$). **a** Full view, **b** detail

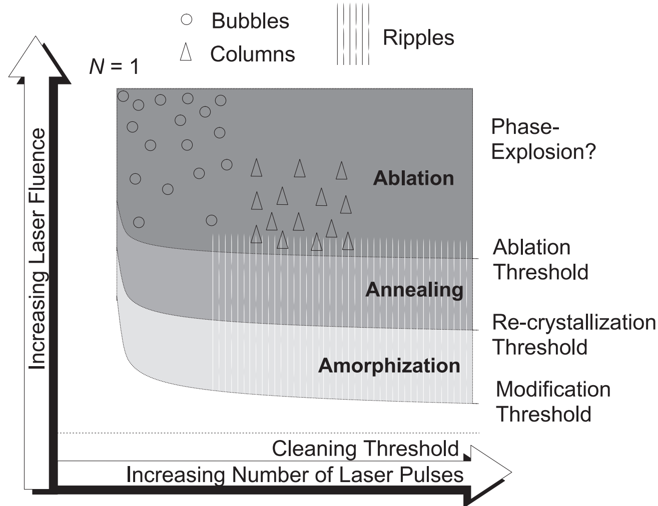


**Fig. 11.** Scheme of the different morphological phenomena after irradiation of the silicon surface with linearly polarized femtosecond laser pulses of typically 100 fs duration

which "guides" the light into the grooves. Therefore, the regions between the columns again act as emitters of ablated material.

A cross-section through a crater (depth $\approx 9\,\mu$m) in silicon obtained after the application of 500 subsequent laser pulses in air ($\lambda = 800$ nm, $\tau = 130$ fs, $\Phi_0 = 0.65\,\mathrm{J/cm^2}$) is shown in Fig. 10a. A detail of the crater wall can be seen in Fig. 10b. Besides an irregular surface morphology and remaining parts of small columns, only a thin thermally or chemically modified layer (depth $< 500$ nm) is visible.

Figure 11 summarizes the different morphological features (bubbles, ripples, microcolumns) formed after irradiation of silicon surfaces with linearly polarized laser pulses for pulse durations of approximately 100 fs.

## 3 Conclusion

We investigated laser-induced modification and ablation of silicon surfaces with laser pulse durations in the range between 5 fs and 400 fs. The multi-pulse ablation threshold fluence is almost constant around $0.2\,\mathrm{J/cm^2}$. We found several physical processes resulting in clearly distinguishable morphological features. These are (from lower to higher fluences) oxidation, amorphization, re-crystallization, the formation of bubbles due to boiling below the surface, and finally ablation. Other features occur while treating the sample with multiple subsequent pulses, namely ripple formation, column growth, and crater formation due to material removal. Although these phenomena can limit the precision of micromachining, there are potential applications of controlled manufactured silicon microcolumns and needles, for example, field-emission sources in the display technology [40]. With respect to the feasibility of using femtosecond pulses for microstructuring of semiconductors one can state that – in contrast to transparent materials – a reduction of the pulse duration below 500 fs does not offer significant advantage, because of the nearly constant ablation threshold fluence and the similarity of the observed surface morphologies.

*Acknowledgements.* We thank Birgid Strauss, Sigrid Benemann, and Marion Männ (all at BAM) for their technical assistance. M.L. acknowledges support by the Austrian Science Foundation (FWF) under grant No. P-12762. We are grateful to Harald Bergner and Gabriele Pfeiffer from the Fachhochschule Jena for help with the AFM.

## References

1. R. Haigh, D. Hayden, P. Longo, T. Neary, A. Wagner: Proc. SPIE **3546**, 477 (1998)
2. M.H. Niemz: *Laser–Tissue Interactions* (Springer, Berlin, Heidelberg 1996)
3. M. Lenzner: Int. J. Mod. Phys. B **13**, 1559 (1999)
4. P.L. Liu, R. Yen, N. Bloembergen, R.T. Hodgson: Appl. Phys. Lett. **34**, 864 (1979)
5. I.W. Boyd, S.C. Moss, T.F. Boggess, A.L. Smirl: Appl. Phys. Lett. **46**, 366 (1985)
6. C.V. Shank, R. Yen, C. Hirlimann: Phys. Rev. Lett. **50**, 454 (1983)
7. J.S. Im, H.J. Kim, M.O. Thompson: Appl. Phys. Lett. **63**, 1969 (1993)
8. A. Cavalleri, K. Sokolowski-Tinten, J. Bialkowski, M. Schreiner, D. von der Linde: J. Appl. Phys. **85**, 3301 (1999)
9. B.N. Chichkov, C. Momma, S. Nolte, F. von Alvensleben, A. Tünnermann: Appl. Phys. A **63**, 109 (1996)
10. Z. Guosheng, P.M. Fauchet, A.E. Siegman: Phys. Rev. B **26**, 5366 (1982) and references therein
11. T.H. Her, R.J. Finlay, C. Wu, S. Deliwala, E. Mazur: Appl. Phys. Lett. **73**, 1673 (1998)
12. D. von der Linde, J. Kuhl, H. Klingenberg: Phys. Rev. Lett. **44**, 1505 (1980)
13. J.A. Van Vechten, R. Tsu, F.W. Saris, D. Hoonhout: Phys. Lett. **74A**, 417 (1979)
14. J.A. Van Vechten, R. Tsu, F.W. Saris: Phys. Lett. **74A**, 422 (1979)
15. I.L. Shumay, U. Höfer: Phys. Rev. **B53**, 15 878 (1996)
16. H.W.K. Tom, G.D. Aumiller, C.H. Brito-Cruz: Phys. Rev. Lett. **60**, 1438 (1988)
17. S.V. Govorkov, I.L. Shumay, W. Rudolph, T. Schröder: Opt. Lett. **16**, 1013 (1991)
18. K. Sokolowski-Tinten, J. Solis, J. Bialkowski, J. Siegel, C.N. Afonso, D. von der Linde: Phys. Rev. Lett. **81**, 3679 (1998)
19. S.I. Anisimov, B.L. Kapeliovich, T.L. Perelman: Sov. Phys. JETP **39**, 375 (1974)
20. P.P. Pronko, P.A. VanRompay, R.K. Singh, F. Qian, D. Du, X. Liu: Mat. Res. Soc. Symp. Proc. **397**, 45 (1996)
21. R. Kelly, A. Miotello: Phys. Rev. E **60**, 2616 (1999)
22. M. Birnbaum: J. Appl. Phys. **36**, 3688 (1965)
23. J.F. Young, J.E. Sipe, H.M. van Driel: Phys. Rev. B **30**, 2001 (1984)
24. G. Herbst, M. Steiner, G. Marowsky, E. Matthias: Mat. Res. Soc. Symp. Proc. **397**, 69 (1996)
25. W. Kautek, J. Krüger: Proc. SPIE **2207**, 600 (1994)
26. F. Sanchez, J.L. Morenza, R. Aguiar, J.C. Delgado, M. Varela: Appl. Phys. Lett. **69**, 620 (1996)
27. A.J. Pedraza, J.D. Fowlkes, D.H. Lowndes: Appl. Phys. Lett. **74**, 2322 (1999)
28. J.E. Rothenberg, R. Kelly: Nucl. Instr. Methods **B1**, 291 (1984)
29. E. van de Riet, C.J.C.M. Nillesen, J. Dieleman: J. Appl. Phys. **74**, 2008 (1993)
30. T.-H. Her, R.J. Finlay, C. Wu, E. Mazur: Appl. Phys. A **70**, 383 (2000)
31. D.H. Lowndes, J.D. Fowlkes, A.J. Pedraza: Appl. Surf. Sci. **154-155**, 647 (2000)
32. S. Sartania, Z. Cheng, M. Lenzner, G. Tempea, Ch. Spielmann, F. Krausz: Opt. Lett. **22**, 1562 (1997)
33. J.M. Liu: Opt. Lett. **7**, 196 (1982)
34. P.B. Corkum, F. Brunel, N.K. Sherman, T. Srinivasan-Rao: Phys. Rev. Lett. **61**, 2886 (1988)
35. Y. Jee, M.F. Becker, R.M. Walser: J. Opt. Soc. Am. B **5**, 648 (1988)
36. J. Bonse, J.M. Wrobel, J. Krüger, W. Kautek: Appl. Phys. A **72**, 89 (2001)
37. O.M. Efimov, K. Gaebel, S.V. Garnov, L.B. Glebov, S. Grantham, M. Richardson, M.J. Soileau: J. Opt. Soc. Am. B **15**, 193 (1998)
38. M. Lenzner, J. Krüger, W. Kautek, F. Krausz: Appl. Phys. A **69**, 465 (1999)
39. J.F. Reintjes, J.C. McGroddy: Phys. Rev. Lett. **30**, 901 (1973)
40. V.V. Zhirnov, E.I. Givargizov, P.S. Piekanov: J. Vac. Sci. Technol., B **13**, 418 (1995)